Supporting Information

Rodriguez-Navarro et al. 10.1073/pnas.1113036109

SI Methods

Animals and Cells. Male C57BL/6 mice (6–8 wk old) were obtained from the Jackson Laboratory. Animals were maintained on the RD (2018, Global 18% Protein Rodent Diet; Teklad), the HFD (D12492, 60% kcal in fat; Research Diets) for 16 wk once they reached 8 wk of age, or the 2% CHOL (2018 + 2% cholesterol TD.01383; Teckland) for 3 wk. At the end of the treatments, some of the animals were starved for 24 h before isolation of lysosomes but they had free access to water. All studies were approved by the Animal Care and Use Committee of the Albert Einstein College of Medicine and followed the National Institutes of Health guidelines on the care and use of animals. Mouse fibroblasts [National Institute of Health (NIH) 3T3] were from the American Type Culture Collection. Cells were maintained in DMEM (Sigma) in the presence of 10% (vol/vol) newborn calf serum. Oleic acid and palmitic acid were conjugated to albumin as described (1), and cells were treated for 24 h.

Chemicals. Sources of chemicals were as described previously (2–5). The antibodies against the cytosolic tail of rat and mouse LAMP-2A and LAMP-2B were prepared in our laboratory (2). The antibodies against mouse LAMP-1 and M6PR were from the Developmental Studies Hybridoma Bank (Iowa University), the antibody against cathepsin D was from Santa Cruz Biotechnology, and the antibodies against hsc70 and hsp90 were from Stressgen. The antibodies against RNase A and cathepsin A were from Rockland Immunochemicals, and the antibodies against GAPDH and ABCB9 were from Abcam. The antibodies against the 19S and 20S proteasome subunits were from BioMol International, the antibody against ubiquitin was from Dako, and the antibody against GFP was from Roche. U18666A was from Sigma, and *N*-butyldeoxygalactonojirimycin was from Toronto Research Company. BODIPY 493/503, cholera toxin and its corresponding antibody, and the Amplex Red cholesterol assay kit were from Molecular Probes (Invitrogen). The high-molecular-weight calibration kit was from Amersham Biosciences.

Isolation of Subcellular Fractions. Mouse liver lysosomes were isolated from a light mitochondrial-lysosomal fraction in a discontinuous metrizamide density gradient, and lysosomal fractions with different activities for CMA were further separated by differential centrifugation as described (6). Lysosomes from cultured cells were isolated as described (7). A crude fraction containing lysosomes and mitochondria was prepared after cell lysis by differential centrifugation (2,500 × *g* for 15 min and 17,000 × *g* for 10 min). Lysosomal matrices and membranes were isolated after hypotonic shock (8). Right after isolation, lysosomes were subjected to centrifugation and the activity of the lysosomal hydrolase β-hexosaminidase was measured in both the pellet (lysosomes) and the supernatant. The enzyme present in the supernatant can originate only from lysosomal disruption because secretion of this enzyme or permeation through the membrane is not possible. Consequently, the percentage of total β-hexosaminidase activity (pellet and supernatant) present outside lysosomes (supernatant) was used to monitor lysosomal breakage. We did not find differences in purity of the fractions or stability of the lysosomal membrane between fed and starved animals or those maintained on the RD, CHOL, or HFD [additional purity information is provided by Koga et al. (9)].

Uptake and Degradation of Substrate Proteins by Isolated Lysosomes. Mouse fibroblast cytosolic proteins were metabolically radiolabeled by incubation with [^{3}H]leucine (2 μCi/mL) at 37 °C for 2 d (6). This pool of radiolabeled cytosolic proteins was incubated in 10 mM 3-(*N*-morpholino) propanesulfonic acid (MOPS) buffer (pH 7.3), 0.3 M sucrose, and 1 mM DTT with intact lysosomes at 37 °C for 30 min (10). Degradation of the radiolabeled substrates was measured after acid precipitation, and proteolysis was expressed as the percentage of the initial acid-insoluble radioactivity (protein) transformed into acid-soluble radioactivity (amino acids and small peptides) at the end of the incubation. Where indicated, lysosomes were disrupted by a hypotonic shock before incubation (8). GAPDH or RNase A was incubated in the MOPS buffer with untreated or protease inhibitor-treated lysosomes as described (10). After incubation for 20 min at 37 °C, lysosomes were collected by centrifugation and samples were subjected to SDS/PAGE and immunoblotted with an antibody against GAPDH or RNase A. Transport was measured, and uptake was calculated as the difference between the amount of substrate associated with lysosomes (protease inhibitor-treated lysosomes) and the amount of substrate bound to their membrane (untreated lysosomes). The inhibitory effect of the diets on the different steps of CMA activity was calculated by the formula [(value RD − value lipid diet)/value RD]·100 and expressed as a percentage.

Measure of CMA Activity in Intact Cells. Stable clones of mouse fibroblasts expressing either of the two CMA reporters (KFERQ-photoactivable mCherry1 or KFERQ-photoswitchable CFP2) (11), treated with oleate or lipid-modifying drugs, as indicated, were photoactivated by light-emitting diode (Norlux) for 10 min with an intensity of 3.5 mA (constant current). After 16 h, cells were fixed with 4% (wt/vol) paraformaldehyde and mounted, and images were acquired with an Axiovert 200 fluorescence microscope (Carl Zeiss Ltd.), subjected to deconvolution with the manufacturer's software, and prepared using Photoshop 6.0 software (Adobe Systems, Inc.). The number of fluorescent puncta per cell was quantified using ImageJ software (National Institutes of Health) in individual frames after thresholding.

Measurement of LAMP-2A Degradation. Rates of degradation of LAMP-2A in the isolated lysosomal membranes were determined by immunoblotting using a specific antibody against the cytosolic tail of LAMP-2A as previously described (3). Briefly, isolated lysosomal membranes were incubated in MOPS buffer at 37 °C, and aliquots were removed and subjected to SDS/PAGE and immunoblotting for LAMP-2A at different times.

Isolation of Detergent-Resistant Lysosomal Membrane Microdomains. Lysosomal membranes (150 μg of protein) from mouse liver were incubated with 1% Triton X-114 in 150 mM NaCl, 50 mM Tris·HCl, and 5 mM EDTA (pH 7.4) (incubation buffer) on ice for 30 min; they were then subjected to centrifugation in a stepwise discontinuous sucrose gradient (5–35%) and centrifuged at 200,000 × *g* for 19 h in an SW-60Ti rotor (Beckman) (12). Four samples of 500 μL collected starting from the detergent-resistant band were subjected to acid precipitation with 10% (vol/vol) trichloroacetic acid and BSA. Precipitates were washed with acetone, resuspended in electrophoresis sample buffer, and subjected to SDS/PAGE and immunoblotting.

Identification of LAMP-2A Multimeric Complexes by Blue-Native Electrophoresis. Lysosomal membranes were solubilized by resuspending them in 20 mM MOPS, 150 mM NaCl, and 0.5% octyl glucoside buffer (except where indicated), and incubating

them for 15 min on ice (13). After centrifugation for 15 min at 16,000 × *g*, the soluble proteins were recovered in the supernatant. The supernatant was supplemented with nonreducing sample buffer and subjected to blue-native electrophoresis using 3–12% (wt/vol) NativePAGE Novex bis-Tris precast gels (Invitrogen), transferred to PVDF membranes, and immunoblotted for LAMP-2A and ABCB9.

Direct Fluorescence and Indirect Immunofluorescence Microscopy. To visualize lipid droplets, cells grown on coverslips were incubated with BODIPY 493/503 for 15 min (14). After extensive washing, cells were fixed with 4% (wt/vol) paraformaldehyde and mounted, and images were acquired with an Axiovert 200 fluorescence microscope, subjected to deconvolution with the manufacturer's software, and prepared using Photoshop 6.0 software. The number of fluorescent puncta per cell was quantified using ImageJ software in individual frames after thresholding. For immunofluorescence, fixed cells were permeabilized and incubated with primary antibody, followed by fluorophore-conjugated secondary antibody, as described previously (11). The percentages of colocalization and colocalized pixels were measured using JACoP (just another colocalization plug-in; Susanne Bolte and Fabrice P. Cordelières) and colocalization plug-ins of ImageJ, respectively.

mRNA Quantification. Total RNA was extracted from mouse livers using the RNeasy Protect Mini Kit (Qiagen) following the manufacturer's instructions and stored at −80 °C until use. The first-strand cDNA was synthesized from 0.5 μg of the total RNA with the SuperScript II RNase H Reverse Transcriptase (Invitrogen) and oligo-$(dT)_{12–18}$ primers. Actin and a region of exon 8 of LAMP-2A were amplified with specific primers (LAMP-2A, 5′-GCAGTGCAGATGAAGACAAC-3′, 5′-GTATGATGGCGCTTGAGAC-3′; actin, 5′-AAGGACTCCTATAGTGGGTGACGA-3′, 5′-ATCTTCTCCAT GTCGTCCCAGTTG-3′; hsc70, 5′-TCTCGGCACCACCTACTCC-3′, 5′-CCCGATCAGACGTTTGGC-3′) using the SYBR green PCR kit (PE Biosystems). Amplification of the LAMP-2A, hsc70, and actin DNA products (120, 196, and 108 bp, respectively) was measured in real-time in a SmartCycler (Cepheid). The expression levels of LAMP-2A in different samples were normalized with respect to those of actin in the same samples.

Lipid Extraction and Analysis. Lipid extracts were prepared using a modified Bligh/Dyer extraction procedure, In brief, membranes from organelle fractions (50 μL) were incubated with methanol and chloroform (2:1 ratio) at 0 °C for 5 min, and lipids were extracted by addition of KCl (1 M, 1:10 ratio) and centrifugation for 2 min at 7,500 × *g* at 4 °C. The organic phase was recovered, and extracted lipids were dried and stored at −80 °C. Lipid extracts were spiked with internal standards and analyzed by liquid chromatography (LC)/MS using multiple reaction monitoring (15–17). The internal standards used included 1,2-dioctanoyl-glycero-3-phosphoinositol (PI; 16:0 ratio; Echelon Biosciences, Inc.), 1,2-dimyristoyl-glycero-phosphoserine (PS; 28:0 ratio), 1,2-dimyristoyl-glycero-3-phosphoethanolamine (PE; 28:0 ratio), 1,2-dimyristoyl-glycero-3-phosphocholine (PC; 28:0 ratio), lauryl-SM (C12-SM), *N*-heptadecanoyl-D-erythro-sphingosine [C17-CER], and D-glucosyl-β1-1′-*N*-octanoyl-D-erythro-sphingosine [C8-glucosyl ceramide (Glu-CER)], which allowed the measurement of PI, PS, PE, plasmalogen-PE, PC, ether-linked-PC, SM, CER, and Glu-CER, respectively. For LC separation, we followed a previously established method using a Luna silica column (3 μm, 2 mm × 150 mm; Phenomenex) with gradient elution of 100% chloroform/methanol/water/ammonia solution (90:9.5:0.5:0.32 vol/vol) changing to 100% chloroform/methanol/water/ammonia solution (50:48:2:0.32 by vol/vol) over 50 min at 0.35 mL/min. Separated lipid classes were quantified via MRM mode on a triple-quadrupole instrument (API 3200; Applied Biosystems). PE/plasmalogen-PE, PI, PS, and PA were detected in negative ionization, whereas CER, GluCER, PC/ether-linked-PC, and SM were detected in positive ionization. Diacylglycerides were analyzed using a modified version of reverse phase high pressure liquid cromatography/electrospray ionization/mass spectrometry (HPLC/ESI/MS) as described previously (15, 17). The remaining lipid classes were measured using previously reported MRM transition pairs and instrument settings (16, 17).

EM. Lysosomal compartments pelleted after centrifugation were fixed in 2.5% glutaraldehyde in sodium cacodylate (SC) [100 mM SC (pH 7.43)] at room temperature for 45 min. The pellet was then rinsed in SC, postfixed in 1% osmium tetroxide in SC followed by 1% uranyl acetate, dehydrated through a graded series of ethanols, and embedded in LX112 resin (LADD Research Industries). Ultrathin sections were cut on a Reichert Ultracut E, stained with uranyl acetate followed by lead citrate, and viewed on a JEOL 1200EX transmission electron microscope at 80 kV.

Measurement of Proteasomal Activity. Proteasomal activity was determined in liver homogenate. Briefly, liver pieces lysed by sonication in 10 mM Tris·HCl (pH 7.8), 1 mM EDTA, 0.5 mM DTT, and 5 mM $MgCl_2$ at 4 °C were centrifuged at 16,000 × *g* for 10 min, and the supernatant was used to measure proteasomal activity directly. The individual proteolytic activities of the proteasome were assayed as their ability to cleave fluorescent peptides specific for each of the activities as follows: 25 μg of liver homogenate was incubated at 37 °C with 1 mM *N*-succinyl-leu-leu-val-tyr-7-amido-4-methylcoumarin (Sigma–Aldrich) to measure peptidyl-glutamyl peptide-hydrolizing activity, with 1 mM *N*-CBZ-leu-leu-glu-β-naphthylamide (Sigma–Aldrich) to measure chymotrypsin-like activity, and with 1 mM BZ-val-gly-arg-AMC (BIOMOL International) to measure trypsin-like activity. Real-time fluorescence was measured at an excitation of 350 nm and an emission of 440 nm for 30 min. Proteasomal inhibitor MG-115 and/or MG-132 was used as a control.

General Methods. Protein concentration was determined by the Lowry method, using BSA as a standard (18). For immunoblotting, the proteins recognized by the specific antibodies were visualized by chemiluminescence methods (Renaissance; NEN–Life Science). Lysosomal enzymatic hexosaminidase and cathepsin A activities were measured as reported previously (7). Quantification of cholesterol was performed using the Amplex Red cholesterol assay kit following the manufacturer's instructions. GAPDH activity was measured with the GAPDH activity kit (ProteinSci).

1. Goldstein JL, Basu SK, Brown MS (1983) Receptor-mediated endocytosis of low-density lipoprotein in cultured cells. *Methods Enzymol* 98:241–260.
2. Cuervo AM, Dice JF (1996) A receptor for the selective uptake and degradation of proteins by lysosomes. *Science* 273:501–503.
3. Cuervo AM, Dice JF (2000) Regulation of lamp2a levels in the lysosomal membrane. *Traffic* 1:570–583.
4. Koga H, Kaushik S, Cuervo AM (2010) Inhibitory effect of intracellular lipid load on macroautophagy. *Autophagy* 6:825–827.
5. Massey AC, Kaushik S, Sovak G, Kiffin R, Cuervo AM (2006) Consequences of the selective blockage of chaperone-mediated autophagy. *Proc Natl Acad Sci USA* 103:5905–5910.
6. Cuervo AM, Dice JF, Knecht E (1997) A population of rat liver lysosomes responsible for the selective uptake and degradation of cytosolic proteins. *J Biol Chem* 272:5606–5615.
7. Storrie B, Madden EA (1990) Isolation of subcellular organelles. *Methods Enzymol* 182:203–225.
8. Ohsumi Y, Ishikawa T, Kato K (1983) A rapid and simplified method for the preparation of lysosomal membranes from rat liver. *J Biochem* 93:547–556.
9. Koga H, Kaushik S, Cuervo AM (2010) Altered lipid content inhibits autophagic vesicular fusion. *FASEB J* 24:3052–3065.
10. Kaushik S, Cuervo AM (2009) Methods to monitor chaperone-mediated autophagy. *Methods Enzymol* 452:297–324.

11. Koga H, Martinez-Vicente M, Macian F, Verkhusha VV, Cuervo AM (2011) A photoconvertible fluorescent reporter to track chaperone-mediated autophagy. *Nat Commun* 2:386.
12. Kaushik S, Massey AC, Cuervo AM (2006) Lysosome membrane lipid microdomains: Novel regulators of chaperone-mediated autophagy. *EMBO J* 25:3921–3933.
13. Bandyopadhyay U, Kaushik S, Varticovski L, Cuervo AM (2008) The chaperone-mediated autophagy receptor organizes in dynamic protein complexes at the lysosomal membrane. *Mol Cell Biol* 28:5747–5763.
14. Singh R, et al. (2009) Autophagy regulates lipid metabolism. *Nature* 458:1131–1135.
15. Dall'Armi C, et al. (2010) The phospholipase D1 pathway modulates macroautophagy. *Nat Commun* 1:142.
16. Chan R, et al. (2008) Retroviruses human immunodeficiency virus and murine leukemia virus are enriched in phosphoinositides. *J Virol* 82:11228–11238.
17. Chan RB, et al. (2012) Comparative lipidomic analysis of mouse and human brain with Alzheimer's disease. *J Biol Chem* 287:2678–2688.
18. Lowry OH, Rosebrough NJ, Farr AL, Randall RJ (1951) Protein measurement with the Folin phenol reagent. *J Biol Chem* 193:265–275.

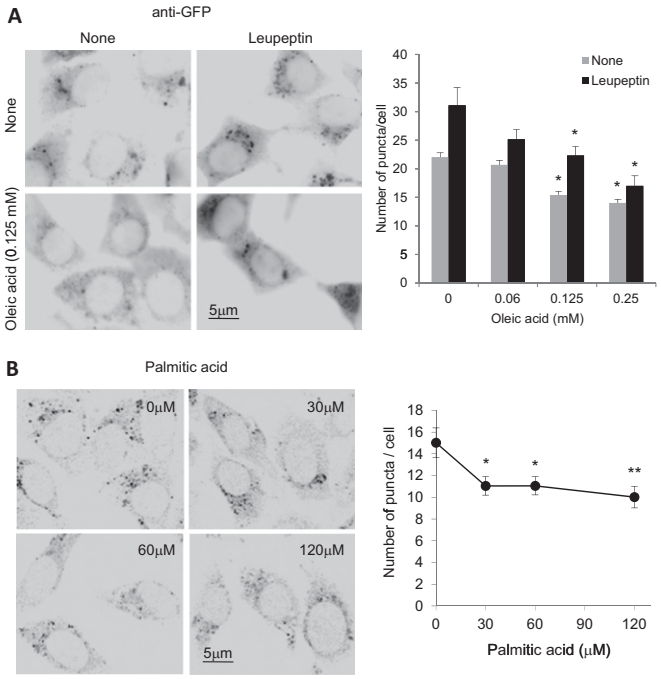

Fig. S1. Effect of treatment with free-fatty acids on CMA activity in fibroblasts. (*A*) Mouse fibroblasts stably expressing a KFERQ-PS-CFP plasmid were exposed to the indicated concentrations of oleic acid in the presence or lack of leupeptin to block lysosomal degradation. Sixteen hours after photoswitching, cells were fixed and immunostained with anti-GFP. (*Left*) Representative fields. (*Right*) Number of fluorescent puncta per cell. (*B*) Mouse fibroblasts stably expressing a KFERQ-PA-mCherry plasmid were exposed to the indicated concentrations of palmitic acid. (*Left*) Representative images 24 h after photoactivation. (*Right*) Number of fluorescent puncta per cell. Values are the mean ± SEM of three different experiments with >50 cells quantified per experiment. *$P < 0.05$ compared with untreated cells. In *A*, the two-way ANOVA, followed by a Bonferroni posttest, showed no interaction between the leupeptin and oleic acid treatments.

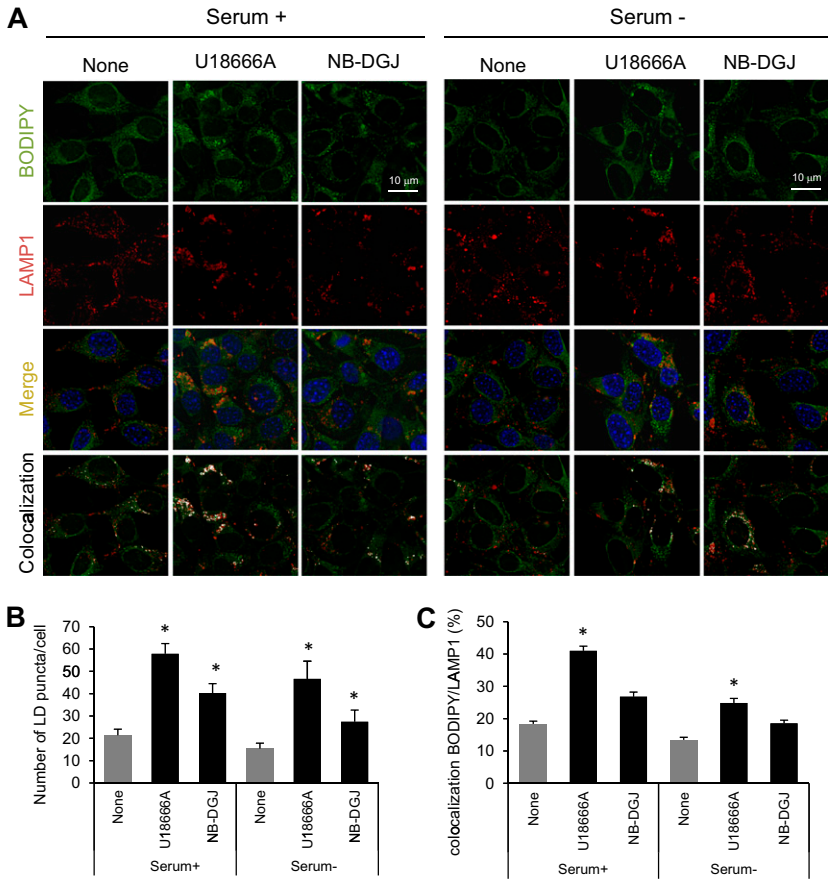

Fig. S2. Effect of different inhibitors of lipid metabolism on intracellular lipid content. Mouse fibroblasts were maintained in the presence or absence of serum, treated with the indicated compounds, and stained with BODIPY and an antibody against LAMP-1. (*A*) Representative images. Individual channels and merged images are shown. (*Bottom*) Colocalization of both fluorophores is highlighted in white. (*B*) Quantification of the number of lipid droplets (LD) per cell after each treatment. (*C*) Percentage of colocalization between BODIPY and LAMP-1 after each treatment. Values are the mean ± SEM of three different experiments with >50 cells quantified per experiment. $*P < 0.05$ compared with untreated cells.

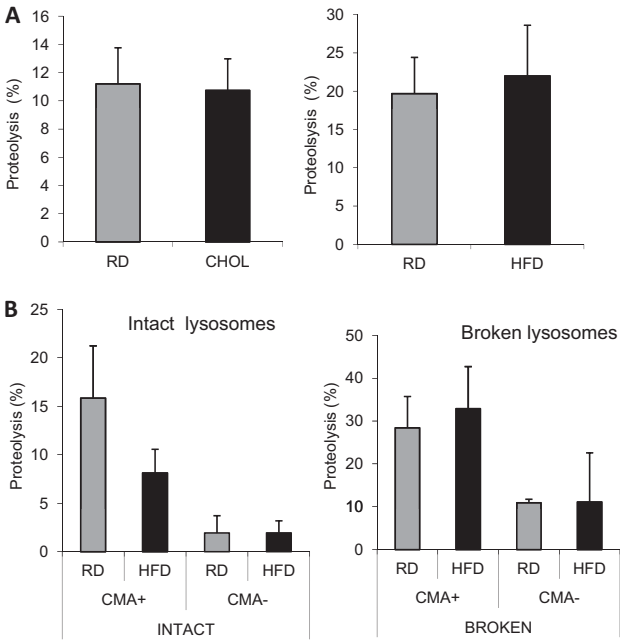

Fig. S3. Effect of lipid challenges on lysosomal proteolytic activity. (*A*) Lysosomes from livers of mice maintained on the RD, CHOL, or HFD were disrupted by a hypotonic shock and incubated with a pool of radiolabeled cytosolic proteins. Proteolysis is expressed as the percentage of acid-insoluble radioactivity transformed into acid-soluble radioactivity at the end of the incubation. Values are the mean ± SEM of three independent experiments. (*B*) Lysosomes with high (CMA+) or low (CMA–) activity for CMA were isolated from livers of mice maintained on the RD or HFD. Intact lysosomes (*Left*) or broken lysosomes disrupted by hypotonic shock (*Right*) were incubated with a pool of radiolabeled proteins, and proteolysis was calculated as in *A*. Values are the mean ± SEM of three experiments.

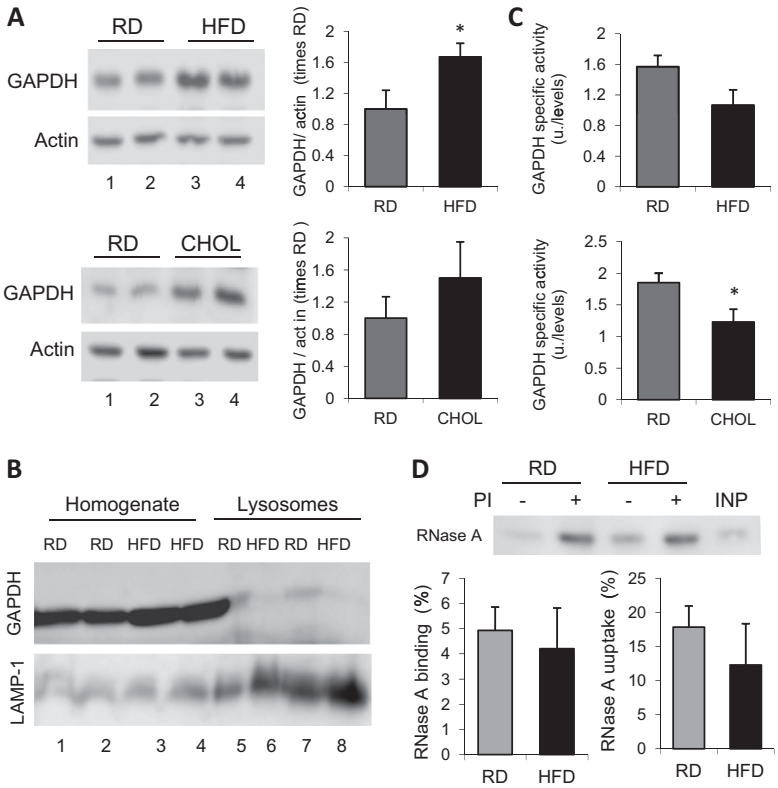

Fig. S4. Effect of high lipid content diets on CMA of different cytosolic proteins. (*A*) Immunoblot for GAPDH of cytosol from livers of mice maintained on the RD, HFD, or CHOL. (*Right*) Quantification of GAPDH levels normalized by actin. (*B*) Immunoblot for GAPDH of homogenates and lysosomes isolated from animals on the RD or HFD. LAMP-1 is shown as a loading control. (*C*) Specific activity of GAPDH (activity corrected for protein levels) in the cytosol of livers from RD-, HFD-, or CHOL-maintained mice. Values are the mean ± SEM of three experiments. (*D*) Lysosomes from mice on the RD or HFD were treated or not treated with a protease inhibitor (PI) as indicated and incubated with RNase A for 20 min at 37 °C in isotonic medium. Lysosomes collected at the end of the incubation by centrifugation were subjected to SDS/PAGE and immunoblotting for RNase A. Uptake was calculated as the amount of RNase A associated with lysosomes treated with protease inhibitors (association) after discounting the amount associated with untreated lysosomes (binding) for each experiment. Values are the range of two independent experiments. $*P < 0.05$ compared with the RD group. INP, input.

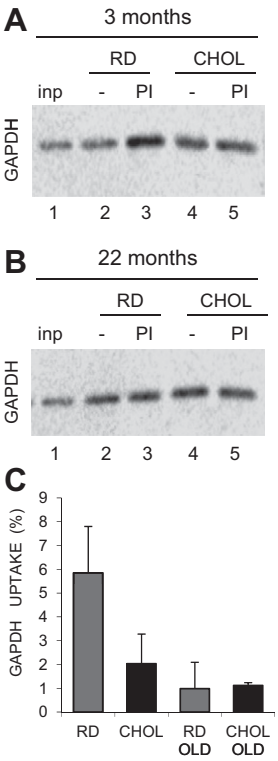

Fig. S5. Effect of lipid challenges on CMA in young and old mice. Lysosomes from 3- and 22-mo-old mice maintained on the RD or 3-wk CHOL were treated or not treated with a protease inhibitor (PI) as indicated and incubated with GAPDH for 20 min at 37 °C in isotonic medium. Lysosomes collected at the end of the incubation by centrifugation were subjected to SDS/PAGE and immunoblotting for GAPDH. *(A* and *B)* Representative immunoblots. (*C*) Uptake was calculated as the amount of GAPDH associated with lysosomes treated with protease inhibitors (association) after discounting the amount associated with untreated lysosomes (binding) for each experiment. Values are the mean ± SEM of three different experiments. inp, input.

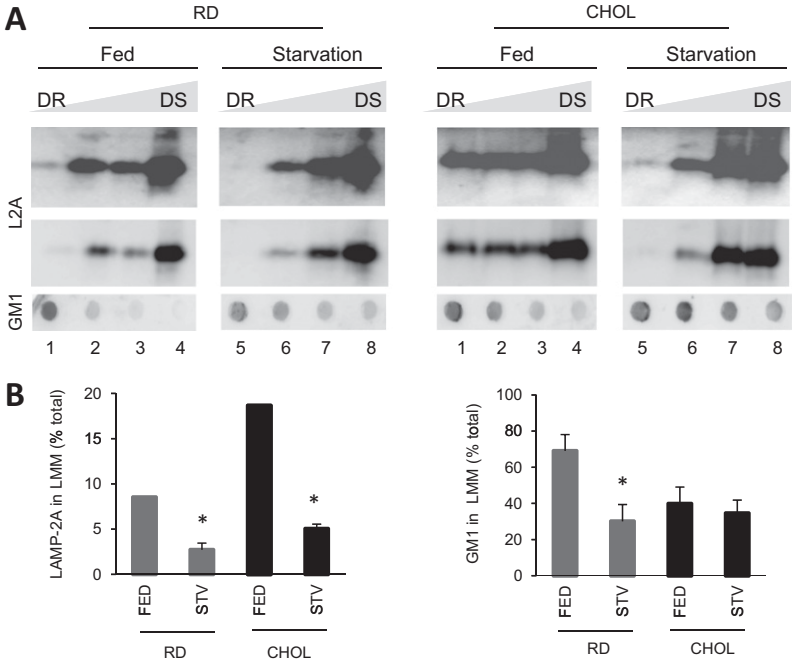

Fig. S6. Changes in the association of LAMP-2A with membrane microdomains in response to high-content lipid diets. Lysosomes from livers of fed mice or mice starved for 24 h maintained on the RD or CHOL were extracted with 1% Triton X-114 and then subjected to flotation in discontinuous sucrose density gradients. Four aliquots collected from the detergent-resistant (DR) to detergent-soluble (DS) region of the gradient were subjected immunoblotting for LAMP-2A (L2A) or dot blot analysis for GM1 using cholera toxin and an antibody against this toxin. (*A*) Representative immunoblots and immunodot blots. (*B*) Densitometric quantification of LAMP-2A (*Left*) and GM-1 (*Right*). Values are expressed as a percentage of the total lysosomal levels and are means of four independent experiments. *$P < 0.05$ compared with fed mice. STV, starved.

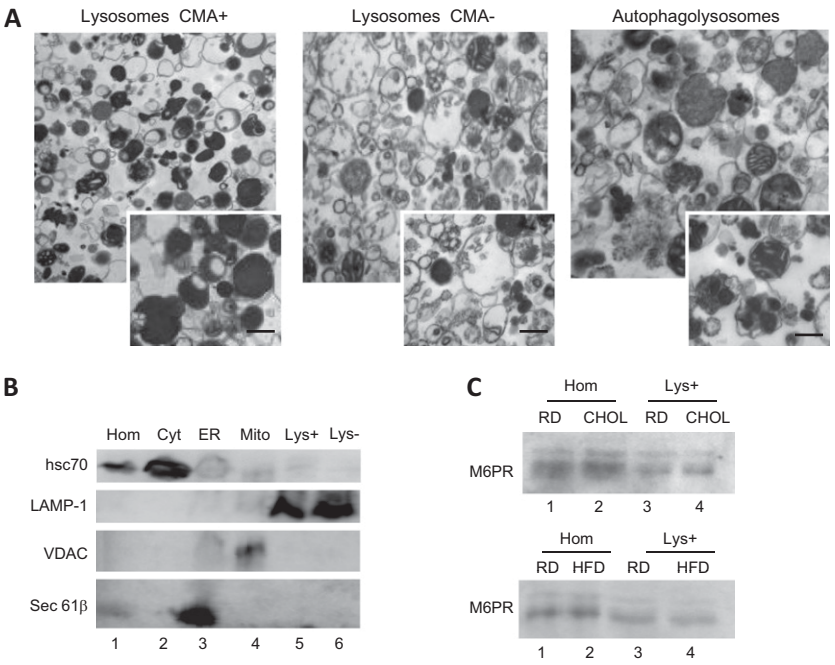

Fig. S7. Morphological and biochemical characterization of the group of lysosomes active for CMA. (*A*) Ultrastructure of lysosomes active for CMA (*Left*), lysosomes inactive for CMA (*Center*), and autophagolysosomes (*Right*). (*Insets*) Higher magnification images. (*B*) Immunoblot for the indicated proteins in fractions isolated from livers of mice starved for 24 h. Cyt, cytosol; ER, endoplasmic reticulum; Hom, homogenate; Lys, lysosomes with high (+) and low (–) CMA activity; Mito, mitochondria. (*C*) Immunoblot for mannose-6-phosphate receptor (M6PR) in homogenates (Hom) and CMA-active lysosomes (Lys+) isolated from animals maintained on the RD, CHOL, or HFD. (Scale bar: 500 nm.)

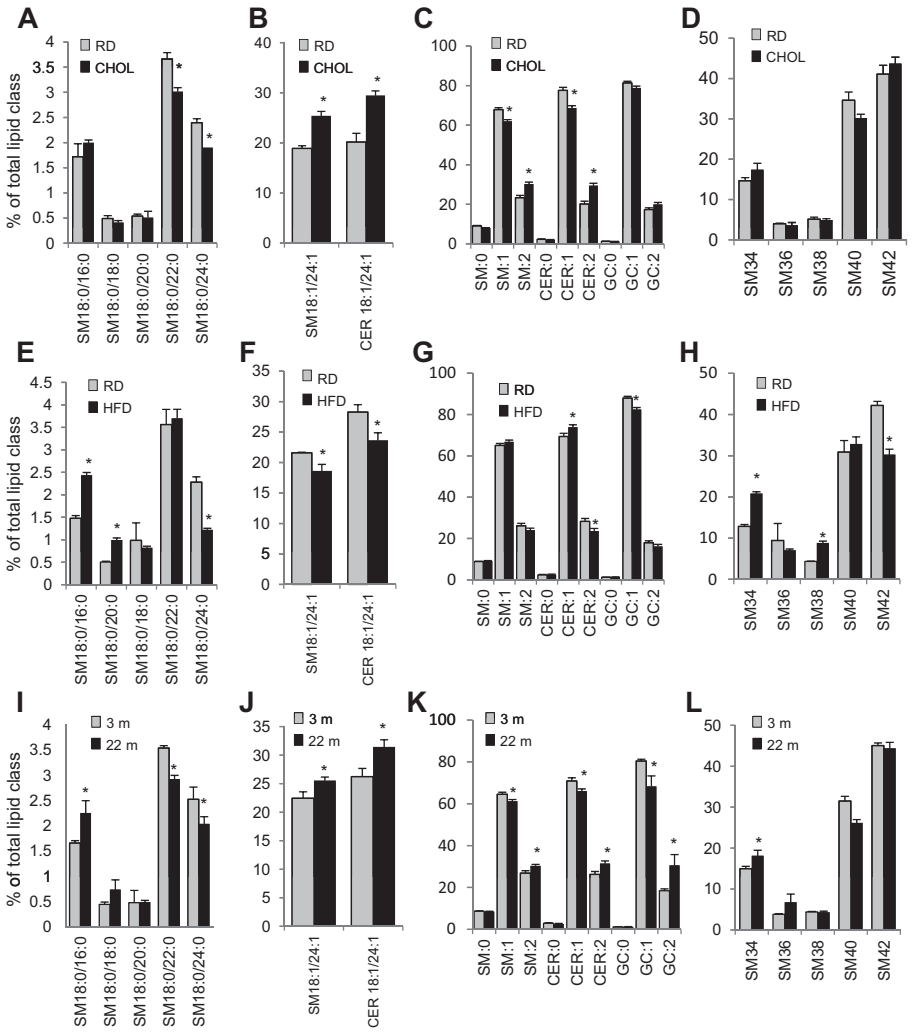

Fig. S8. Glycosphingolipid changes in the lysosomal membrane in response to dietary lipids and aging. Lysosomal membranes from livers of mice maintained on the RD, CHOL (*A–D*), or HFD (*E–H*) or from 3- and 22-mo-old mice (*I–L*) were subjected to comparative lipidomic analysis. Graphs show the percentage of saturated SM, unsaturated SM, CER, and glucoceramide (GC) relative to the total SM, CER, and GC in the samples. Values are the mean ± SEM from five different experiments. *$P < 0.05$ compared with the RD-maintained (*A–H*) or 3-mo-old (*I–L*) mice.

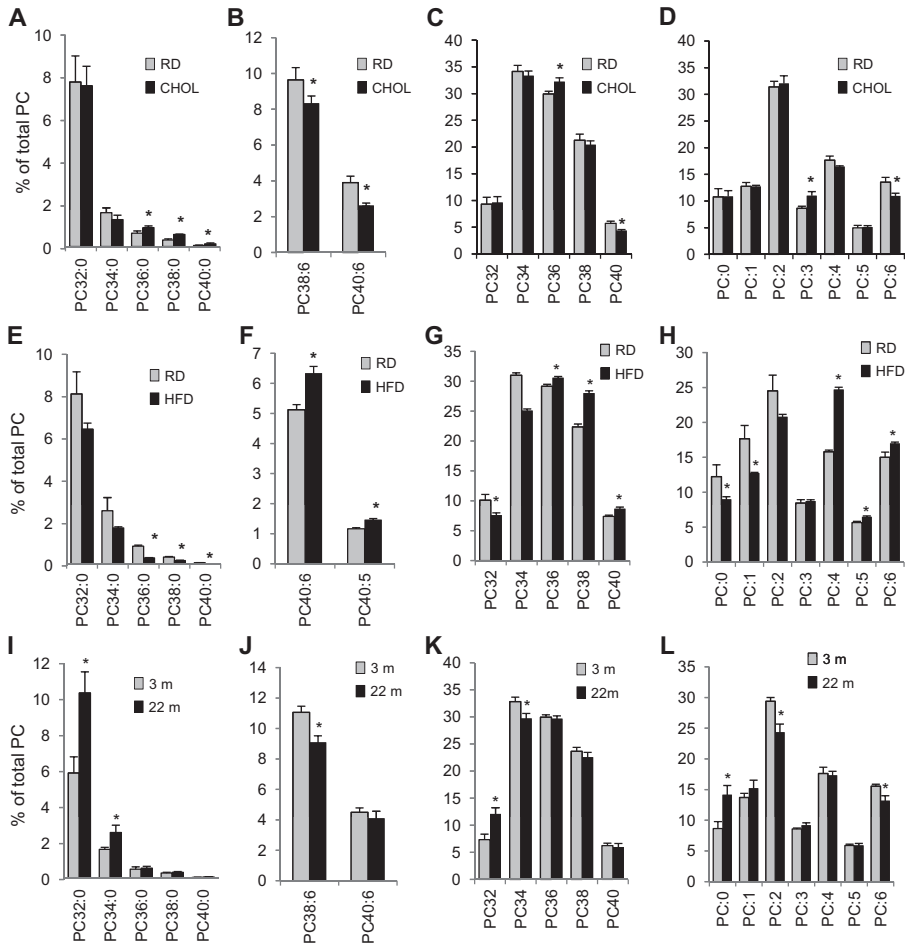

Fig. S9. PC changes in the lysosomal membrane in response to dietary lipids and aging. Lysosomal membranes from livers of mice maintained on the RD, CHOL (*A–D*), or HFD (*E–H*) or from 3- and 22-mo-old mice (*I–L*) were subjected comparative lipidomic analysis. Graphs show the percentage of saturated, unsaturated, and different acyl chain-length PC relative to the total PC in the samples. Values are the mean ± SEM from five different experiments. $*P < 0.05$ compared with RD-maintained (*A–H*) or 3-mo-old (*I–L*) mice.

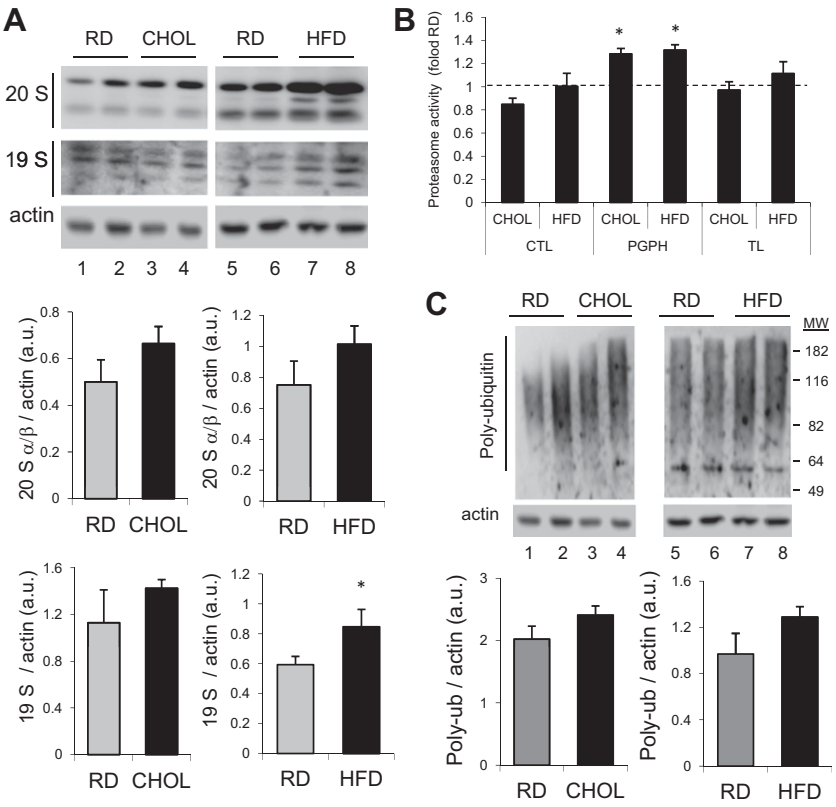

Fig. S10. Changes induced by dietary lipids in the ubiquitin/proteasome system. (*A*) Immunoblot for the subunits of the 19S and 20S proteasomes in livers of mice maintained on the RD, CHOL, and HFD. (*Lower*) Densitometric quantification of three immunoblots as the one shown here. Values are expressed in arbitrary units (a.u.) and are corrected for actin. (*B*) Catalytic activities of the 20S proteasome measured with specific fluorescent substrates in the same livers. CTL, chymotrypsin-like; PGPH, peptidyl-glutamyl peptide hydrolyzing activity; TL, trypsin-like. (*C*) Immunoblot for ubiquitin in the same livers. (*Lower*) Densitometric quantification of three immunoblots as the one shown here. Values are expressed in arbitrary units and are corrected for actin. Poly-ub, polyubiquitin. Values are the mean ± SEM from three different experiments. $^*P < 0.05$ compared with the RD.